



ELSEVIER

Journal of Nuclear Materials 290–293 (2001) 1128–1133

Journal of
nuclear
materials

www.elsevier.nl/locate/jnucmat

Modeling of particulate production in the SIRENS plasma disruption simulator

J.P. Sharpe^{a,*}, B.J. Merrill^a, D.A. Petti^a, M.A. Bourham^b, J.G. Gilligan^b

^a Fusion Safety Program, Idaho National Engineering and Environmental Laboratory, P.O. Box 1625, Ms 3860, Idaho Falls, ID 83415-3860, USA

^b Department of Nuclear Engineering, North Carolina State University, Raleigh, NC 27695-7909, USA

Abstract

Modeling of the complex interplay among plasma physics, fluid mechanics, and aerosol dynamics is critical to providing a detailed understanding of the mechanisms responsible for particulate production from plasma–surface interaction in fusion devices. Plasma/fluid and aerosol models developed for analysis of disruption simulation experiments in the SIRENS high heat flux facility integrate the necessary mechanisms of plasma–material interaction, plasma and fluid flow, and particulate generation and transport. The model successfully predicts the size distribution of primary particulate generated in SIRENS disruption-induced material mobilization experiments. © 2001 Elsevier Science B.V. All rights reserved.

Keywords: Disruption; Modelling

1. Introduction

A complete description of plasma–material interactions requires a model that describes the underlying mechanisms responsible for generation of particulate (i.e. dust or aerosol). Plasma exposure to adjacent plasma-facing components has been found to erode and mobilize debris from its surface at a rate dependent on the length and intensity of exposure. Accidental or uncontrolled release of plasma energy in a large fusion reactor may not only have a severe effect on the structural integrity of plasma-facing surfaces, but also can mobilize large amounts of particulate. This dust is likely radioactive, chemically reactive, and toxic, thereby posing important design, operational, and safety constraints [1,2]. Such a model will be useful in accurately determining the inventory of dust in a fusion device, which is essential for a defensible safety analysis.

Particulate from existing fusion facilities has been collected and characterized [3–6] in an effort to compile operational data to guide the definition of dust safety limits in future large fusion experiments, such as ITER [7]. Additionally, controlled plasma exposure experiments using fusion-relevant materials (e.g. W, Cu, SS316, C, and mixtures thereof) have been performed with the SIRENS high heat flux facility at North Carolina State University, Raleigh, NC [8,9]. This facility utilizes an electrothermal plasma source section that is suitable for simulating tokamak disruption heat loads [10]. Material eroded from the target surface is similar to the dust generated by disruption-induced mobilization. The experiment's configuration allowed mobilized material to move away from the plasma-exposed surface and into a large expansion chamber. Particulate formed as a result of this process was collected from the chamber and analyzed for characteristics such as size distribution, morphology, and chemical composition. Based on relevant mechanisms of plasma/fluid transport and aerosol generation, growth, and transport, a one-dimensional (1-D) model has been developed to simulate particulate mobilization in the SIRENS experiments. The development of this model is outlined in Section 2.

* Corresponding author. Tel.: +1-208 526 9830; fax: +1-208 526 2930.

E-mail address: sharjp@inel.gov (J.P. Sharpe).

In Section 3, results of experiment simulations are presented and the model results are compared to measured particle size distributions.

2. Model description

Numerical models have been developed to understand the underlying physical processes governing particulate mobilization experiments performed with the SIRENS facility. The plasma source configuration and fluid flow geometry, shown in Fig. 1, are of 1-D coaxial arrangement very typical of electrothermal plasma sources. The cylindrical plasma source section (radius of 0.2 cm and length of 6 cm) contains a sleeve composed of sample material, and the present model allows only a single component plasma/fluid consisting of the test material. Electric current (~ 30 kA) applied to the source section by an external pulsed power system is assumed to be uniformly distributed over the plasma column in the source section. Radiant energy from the plasma heats and vaporizes the sample surface, thereby mobilizing material in a manner similar to a disruption heat load [10]. Attached to the plasma source section is a large expansion chamber (radius of 9.0 cm and length of 76 cm). A region of linearly expanding radii are used in the model to connect the small source section to the large chamber in an attempt to capture the multi-dimensional effects associated with the sudden expansion of the experiment with the 1-D model. This region is not part of the experiment but is required to keep the model reasonably simple.

2.1. Plasmasfluid model

Material vaporized from the sample sleeve in the source section during the plasma discharge (~ 50 μ s) [8] comprises the fluid that expands into the chamber and

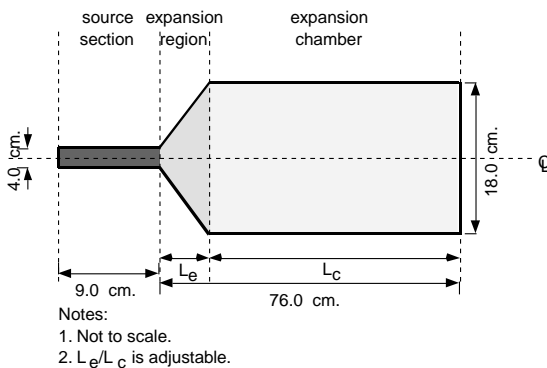


Fig. 1. Model configuration of the experiment source section and expansion chamber.

generates the particulate of interest. Electric current in the source section generates partially ionized plasma from this material. As the fluid exits the source section, recombination occurs and the fluid is no longer ionized. Therefore multi-species fluid conservation equations are written to describe electron, ion, and neutral population densities, temperatures, and velocities. In the present model, these equations are 1-D and represent fluid flow along the axis of the SIRENS experiment.

Conservation of total mass is described with equations of continuity of plasma species. For a plasma of a single chemical component a , there are Z possible ionic charge states, one neutral population, and an electron population, giving $Z + 2$ state populations to be conserved. Thus the continuity equation for a general population n_a^q is

$$\frac{\partial}{\partial t} (n_a^q) + \frac{1}{A} \frac{\partial}{\partial z} (A n_a^q v_a^q) = S_a^q, \quad (1)$$

where q is the species charge and ranges from 0 (neutrals) to Z , A the cross-sectional area, and v_a^q is the species axial velocity. The right-hand side (S_a^q) is a source/sink term describing exchange of particles between the various populations. A general charge state population will have sources and sinks due to electron impact ionization and radiative recombination. The species' densities and collisional rate coefficients, which vary with electron temperature and density, give the reaction rates among various species. The source term in the neutral's continuity equation has an additional term that represents the ablation rate of neutrals from the source section sleeve [11]:

$$S_{\text{wall}} = \frac{f_{\text{vs}} Q_{\text{rad}} N_A}{h_{\text{sub}} (\text{MW})}, \quad (2)$$

where f_{vs} is a 'vapor shielding' factor used to account for protection of the ablating wall provided by the gas layer adjacent to the wall [11]. Q_{rad} is the plasma radiation energy density, N_A Avagadro's number, h_{sub} the target material sublimation enthalpy, and (MW) represents the sample material's molecular weight. With a large neutral population density and low ionization fraction typical of an electrothermal plasma, the axial velocity of charged species may be neglected, leaving only the neutrals to carry flow momentum. A final requirement for mass conservation is charge continuity, such that the electron density n_e is given by

$$n_e = \sum_{q=0}^Z q n_a^q. \quad (3)$$

In this multi-species plasma/fluids model, energy must also be conserved for each species, and all relevant mechanisms of energy exchange among the species must be included. The electron energy equation used in this model is [11]

$$\frac{\partial}{\partial t} \left[\frac{3}{2} n_e T_e \right] = -Q_{\text{Rad}} + \eta j^2 - \kappa_i (T_e - T_i) - \kappa_0 (T_e - T_0) + Q_e^{\text{other}}, \quad (4)$$

where T_e , T_i and T_0 are electron, average ion, and neutral temperatures, respectively, η the plasma resistivity due to electron–ion and electron–neutral collisions, j the source current density, and the terms κ_i and κ_0 are ion and neutral equilibration factors [11]. The average ion energy equation used in this model is given as [11]

$$\frac{3}{2} \frac{\partial}{\partial t} [n_a^i T_i] = \kappa_i (T_e - T_i) + Q_i^{\text{other}}, \quad (5)$$

where n_a^i is the total ion density. The neutral energy equation of this model is [11]

$$\begin{aligned} \frac{\partial}{\partial t} \left(\frac{3}{2} n_a^0 T_0 \right) + \frac{1}{A} \frac{\partial}{\partial z} \left(\frac{5}{2} A n_a^0 T_0 v_a^0 \right) \\ = \frac{v_a^0}{A} \frac{\partial}{\partial z} (A n_a^0 T_0) + \kappa_0 (T_e - T_0) + Q_0^{\text{other}}. \end{aligned} \quad (6)$$

The source terms Q_e^{other} , Q_i^{other} , and Q_0^{other} represent species energy exchange from ionization and recombination events [11].

The final conserved quantity in this model is neutral momentum. Electron and ion momenta are neglected because the large neutral population dominates flow momentum in electrothermal plasmas [12]. The axial momentum equation for the neutral species is [11]

$$\frac{\partial}{\partial t} (n_a^0 v_a^0) + \frac{1}{A} \frac{\partial}{\partial z} (A n_a^0 v_a^0 v_a^0) + \frac{\partial}{\partial z} \left(\frac{1}{m} n_a^0 T_0 \right) = 0, \quad (7)$$

where m is the neutral species mass. This equation, along with the ideal gas equation of state to relate neutral temperature and pressure, completes the plasma/fluid transport model.

2.2. Aerosol growth and transport model

Generation of particulate in the SIRENS experiment results from supersaturation of vapor as it expands and cools in the chamber. Aerosol particles are formed when the vapor condenses to relieve supersaturation, and the nucleated particles grow in size by diffusional condensation and coagulation. An aerosol population is usually described by its particle size distribution. The aerosol general dynamic equation (GDE) is used to calculate the dynamics of the particle size distribution [13]

$$\begin{aligned} \frac{\partial n}{\partial t} t + \frac{\partial}{\partial z} (n v_a^0) = \nabla \cdot (D \nabla \cdot n) + \left[\frac{\partial n}{\partial t} \right]_{\text{growth,homo}} \\ + \left[\frac{\partial n}{\partial t} \right]_{\text{growth,hetero}} + \left[\frac{\partial n}{\partial t} \right]_{\text{coag}} - \nabla \cdot \bar{c} n, \end{aligned} \quad (8)$$

where n represents the particulate density distribution function and D is the diffusion coefficient for Brownian motion of the aerosol particles. The bracketed terms represent the rate of change in the aerosol size distribution due to particulate growth (homogeneous and heterogeneous) and particulate coagulation. The final term on the right-hand side represents the rate at which aerosol particles are removed from the system because of external forces, such as gravitational settling. At present, the model excludes aerosol transport by diffusion and aerosol removal by external forces because these processes are slow compared to particulate convection to and deposition on the chamber wall [11]. Also, rates of growth by diffusional deposition of vapor on nearby particulate as well as coagulation dominate until the vapor is depleted at saturation and equilibrium is reached [14].

Aerosol that forms directly from a particulate-free supersaturated vapor does so by homogeneous nucleation at a rate given by [11]

$$\begin{aligned} \left[\frac{\partial n}{\partial t} \right]_{\text{growth,homo}} = \left(\frac{P_{\text{sat}}}{kT} \right)^2 \left(\frac{2\sigma m}{\pi} \right)^{1/2} \frac{S^2}{\rho_l} \\ \times \exp \left[-\frac{\pi \sigma d_{\text{crit}}^2}{3kT} \right] \delta(V_{\text{crit}}), \end{aligned} \quad (9)$$

where P_{sat} is the vapor saturation pressure over an infinite flat surface, k the Boltzmann constant, T the local (neutral) vapor temperature, σ the surface tension of a condensed droplet of the material, S the saturation ratio (defined as $S = P/P_{\text{sat}}$ with P representing the local vapor pressure), and ρ_l is the liquid phase density of the material. The two remaining parameters, d_{crit} and V_{crit} , are the critical size and volume at which the condensation and evaporation rates of the cluster are equal [13]:

$$d_{\text{crit}} = \frac{4\sigma m}{\rho_l kT \ln S}, \quad \text{and} \quad V_{\text{crit}} = \frac{\pi}{6} d_{\text{crit}}^3. \quad (10)$$

The delta function in Eq. (9) is necessary to place the nucleated aerosol at the correct position in particulate volume space when describing the rate of change of the particulate distribution function.

The aerosol growth rate by heterogeneous nucleation is given as [13]

$$\left[\frac{\partial n}{\partial t} \right]_{\text{growth,hetero}} = -\frac{\partial I}{\partial(V)} = -\frac{\partial}{\partial(V)} \left(n \frac{\partial}{\partial t} (V) \right), \quad (11)$$

where I is the current through particulate volume space (V), or the product of number frequency and aerosol growth rate [13]:

$$\frac{\partial}{\partial t} (V) = 2\pi \left(\frac{\pi}{6} \right)^{1/3} \frac{(S-K) P_{\text{sat}} D d_p}{kT} V_{\text{mol}} F. \quad (12)$$

In this expression, d_p is the diameter of the aerosol particle, and V_{mol} is the volume of a single molecule of

the condensing vapor species. K is a factor that accounts for the Kelvin effect on the local vapor saturation pressure. Finally, F is responsible for adjusting the growth rate expression for the range of particulate sizes [13].

Aerosol particle-to-particle collisions (from Brownian motion) affect the overall size distribution since two particles are removed and one particle with the sum of the volumes is added. This process is called coagulation and changes the size distribution at a rate given by [13]

$$\left[\frac{\partial n}{\partial t} \right]_{\text{coag}} = \frac{1}{2} \int_0^V \beta(V^*, V - V^*) n(V^*) n(V - V^*) dV^* - \int_0^\infty \beta(V, V^*) n(V) n(V^*) dV^*, \quad (13)$$

where the collision frequency function $\beta(V, V^*)$ is given by [15]

$$\beta(V, V^*) = 2\pi(D + D^*)(d_p + d_p^*)F_{\text{coag}}. \quad (14)$$

F_{coag} corrects the expression for all ranges of particle sizes [15].

2.3. Model integration

The premise of integrating the plasma/fluids and aerosol models is that the GDE and fluid equations form a complete equation set coupled by the parameters of vapor (neutral) temperature T , pressure P , and velocity v , and particle nucleation and growth rates. For given T and P , nucleation and growth rates of particles of different sizes may be determined. Similarly, if growth rates are known for a given particle size distribution, a mass loss term is calculated for the equation of continuity of neutral mass, which is solved simultaneously with neutral energy and momentum to give values of vapor T , P , and v . The method used to couple the calculation of these parameters solves the aerosol GDE explicitly over one flow time step with known vapor parameters. Calculation of a corresponding vapor mass sink is performed, and the value is used in the next flow time step to solve for new vapor parameters [11]. The calculation is advanced based on these new values. This solution technique has been benchmarked with standard analytical problems of fluid and aerosol dynamics [11].

3. Simulation results

The plasma/fluid and aerosol models presented in Section 2 have been used to simulate particle production experiments in SIRENS. Calculations were performed for an experiment test with a copper sample exposed to a 4.6 kJ plasma discharge. The calculation predicts that 86 mg of mass is eroded from the sample sleeve and is available for generation of particulate. Electron, ion,

and neutral temperatures were found to equilibrate rapidly after initiation of the discharge in the model. This result concurs with the assumption of local thermodynamic equilibrium in modeling electrothermal plasmas [12]. The average plasma temperature measured during the discharge was 1.34 eV, whereas the average discharge temperature calculated by the model was 1.25 eV. Fig. 2 shows the corresponding chamber pressure at various times in the simulation. These profiles clearly indicate the propagation of a pressure pulse into the chamber. The pulse arrives at the closed end of the chamber (0.76 m) at 500 μs and is reflected. At 2000 μs , the pulse has reached the source/chamber interface and is again reflected. The simulation ends at 3600 μs when the pressure profile has become nearly uniform at a value of 100 Pa. Formation and growth of particulate occur throughout the simulation in regions where the local pressure exceeds the saturation pressure. At completion of the simulation (3600 μs), the vapor has radiatively cooled to a temperature of 0.04 eV, a value slightly greater than the chamber wall boundary condition of 0.025 eV. This vapor temperature and pressure result in a total vapor mass of 32 mg, and the remaining 54 mg is equivalent to the total mass of generated particulate. Fig. 3 shows vapor velocities at various times during the simulation. As the vapor is reflected from the closed end of the chamber, flow direction is reversed, as indicated by the negative values of velocity at times following reflection. Particulate generated during the simulation is transported throughout the chamber with the velocities indicated in the figure. With increasing time in the simulation, the vapor slows by viscous dampening and the calculated velocity becomes nearly zero. Convective transport is responsible for deposition of particulate on the chamber boundary. The size distribution of this deposited particulate is compared in

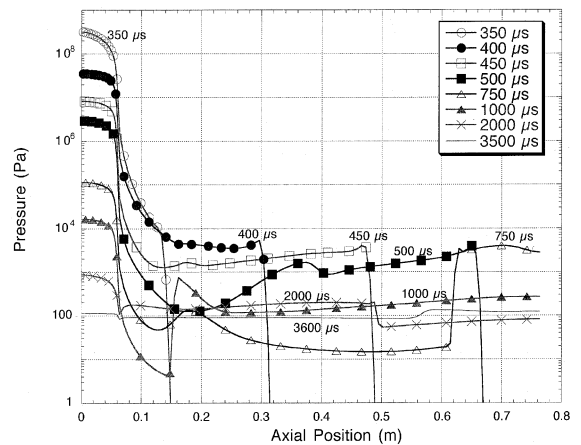


Fig. 2. Calculated chamber pressure profiles for the copper experiment test.

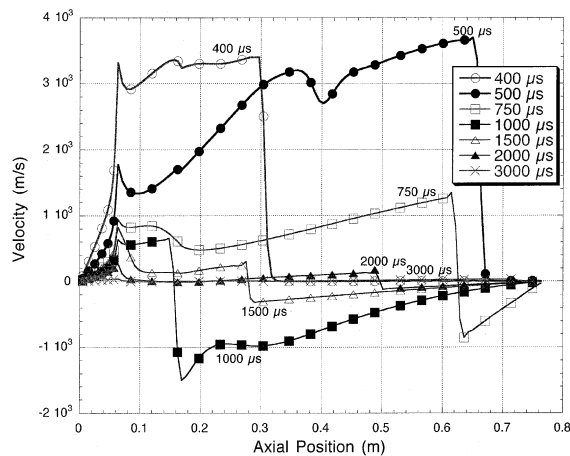


Fig. 3. Calculated vapor velocity profiles for the copper experiment test.

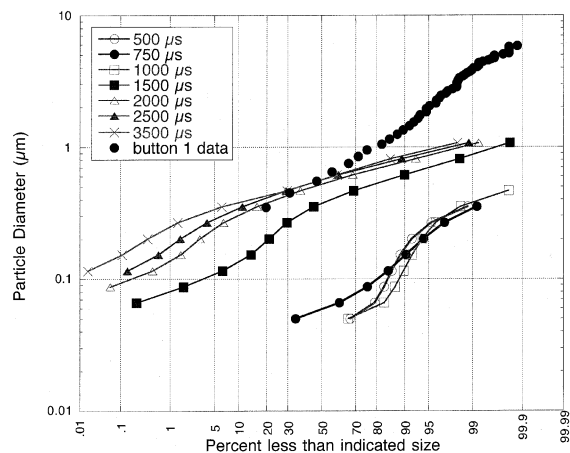


Fig. 4. Predicted and measured particulate size distributions for a chamber region 20 cm from the source section exit.

Fig. 4 to the measured size distribution of particulate collected from the experiment. The calculated particulate size is very small and the concentration is low at times early in the simulation. As time progresses, the particulate grows and approaches the size distribution of approximately 70% of the collected particulate. Deviation from the remaining 30% of the measured distribution results from a source of large ($>1 \mu\text{m}$) particulate in the experiment that is not included in this model. The measured mass loss from the copper sample sleeve in this experiment was 450 mg – a value much greater than the 85 mg predicted with only ablation acting to mobilize material, as is assumed in the model. Larger particulate, and hence greater mobilized mass, likely result from removal of material from a molten layer at the exposed surface of the sample sleeve [11]. Table 1 summarizes the

Table 1

Summary of comparison of predicted and measured particulate sizes for a copper test

Location	CMD ^a and GSD ^a	
	Measured	Calculated ^b
Region I (0–0.25 m)	0.66 μm	0.67 μm
	1.77	0.65
Region II (0.25–0.42 m)	–	0.62 μm
	–	0.58
Region III (0.42–0.58 m)	0.78 μm	0.62 μm
	2.13	0.58
Region IV (0.58–0.76 m)	0.55 μm	0.78 μm
	2.38	0.74

^a CMD = count median diameter, GSD = geometric standard deviation.

^b Based on distribution calculated at 3600 μs , i.e. the end of the simulation.

comparison of predicted and measured size distribution parameters for various locations within the expansion chamber. Count median diameters (CMD) compare reasonably well (within 30%), whereas the geometric standard deviations (GSD) are much larger for the measured distributions. A greater population of larger particles in the measured distribution accounts for the significant differences in GSDs. Similarity in the predicted and measured values of CMDs indicates that a large number of the measured particles were formed by the mechanisms of nucleation and growth included in the model. These mechanisms are responsible for the observed size distribution of the primary particulate [11].

4. Conclusion

Modeling of the complex interplay among plasma physics, fluid mechanics, and aerosol dynamics is critical to providing a detailed understanding of the mechanisms responsible for particulate production from plasma–surface interaction in fusion devices. Such a model is essential for the design and safety analysis of a future large fusion reactor because presently no such devices exist from which relevant data may be obtained. The plasma/fluid and aerosol models outlined in this paper may serve as a foundation for calculation of particulate mobilization in future fusion reactors because they successfully integrate the necessary mechanisms of plasma–material interaction, plasma and fluid flow, and particulate generation and transport.

The integrated model was demonstrated with reasonable success by simulating the particulate production experiments in SIRENS. Calculated median particulate sizes generally agreed with measured median sizes, although the measured particulate included a portion of the population at sizes larger than the predicted and

measured median values. The model was successful in predicting the size distribution of primary particulate in the measured particulate population.

Future work with this model is directed at adaptation to the tokamak geometry for the purpose of evaluating the total inventory of tokamak dust.

Acknowledgements

This work was supported by the US Department of Energy, Office of Energy Research, Idaho Operations Office, under DOE Contract DE-AC07-99ID13727.

References

- [1] D.A. Petti, K.A. McCarthy, *Fus. Technol.* 37 (2000) 1.
- [2] J. Winter, *Plasma Phys. Control. Fus.* 40 (1998) 1201.
- [3] W.J. Carmack et al., *Fus. Eng. Des.* 39 (1998) 477.
- [4] S.V. Gorman, W.J. Carmack, P.B. Hembree, *Fus. Technol.* 34 (1998) 745.
- [5] W.J. Carmack et al., ITER Engineering Design File ITER/US/98/TE/SA-8, April 1998.
- [6] W.J. Carmack, Nova Dust Particulate Characterization (March and April 1999 Opening), INEEL/EXT-99-00793, Fusion Safety Program, Idaho National Engineering and Environmental Laboratory, September 1999.
- [7] S.J. Piet et al., in: Proceedings of the 17th IEEE/NPSS Symposium on Fusion Engineering, San Diego, CA, 6–10 October 1997, Institute of Electrical and Electronic Engineers (1997).
- [8] J.P. Sharpe, M.A. Bourham, J.G. Gilligan, in: Proceedings of the 17th IEEE/NPSS Symposium on Fusion Engineering, San Diego, CA, 6–10 October 1997, Institute of Electrical and Electronic Engineers (1997).
- [9] J.P. Sharpe, M.A. Bourham, J.G. Gilligan, *Fus. Technol.* 34 (1998) 634.
- [10] J.G. Gilligan, M.A. Bourham, *Fus. Energy* 12 (1993) 113.
- [11] J.P. Sharpe, Ph.D. thesis, North Carolina State University, Raleigh, NC, 2000.
- [12] A. Loeb, Z. Kaplan, *IEEE Trans. Magnetics* 25 (1989) 342.
- [13] S.K. Friedlander, *Smoke, Dust, and Haze: Fundamentals of Aerosol Behavior*, Wiley, New York, 1977.
- [14] D.A. Powers, J.E. Brockman, A.W. Silver, NUREG/CR-4308, July 1986.
- [15] C.J. Wheatley, NUREG/CR-5162, August 1988.